Extended VHE γ-ray emission towards SGR1806-20, LBV 1806-20, and stellar cluster Cl* 1806-20

HESS 2 collaboration; Abdalla, H.; Abramowski, A.; Aharonian, F.; Ait Benkhali, F.; Akhperjanian, A. G.; Angüner, E. O.; Arrieta, M.; Aubert, P.; Backes, M.; Balzer, A.; Barnard, M.; Becherini, Y.; Becker Tjus, J.; Berge, D.; Bernhard, S.; Bernlöhr, K.; Birsin, E.; Blackwell, R.; Böttcher, M.; Boisson, C.; Bolmont, J.; Bordas, P.; Bregeon, J.; Brun, F.; Brun, P.; Bryan, M.; Bulik, T.; Capasso, M.; Carr, J.; Casanova, S.; Chakraborty, N.; Chalme-Calvet, R.; Chaves, R. C. G.; Chen, A.; Chevalier, J.; Chrétien, M.; Colafrancesco, S.; Cologna, G.; Condon, B.; Conrad, J.; Couturier, C.; Cui, Y.; Davids, I. D.; Degrange, B.; Deil, C.; Prokoph, H.; Salek, D.; Simoni, R.; Vink, J.

DOI
10.1051/0004-6361/201628695

Publication date
2018

Document Version
Final published version

Published in
Astronomy & Astrophysics

A&A 612, A11 (2018)
DOI: 10.1051/0004-6361/201629695

H.E.S.S. phase-I observations of the plane of the Milky Way

Astronomy & Astrophysics
Special issue

Extended VHE γ-ray emission towards SGR1806−20, LBV 1806−20, and stellar cluster Cl* 1806−20

H.E.S.S. Collaboration, H. Abdalla[1], A. Abramowski[2], F. Aharonian[3,4,5], F. Ait Benkhali[3], A. G. Akhperjanian[6,5], E. O. Angüner[7], M. Arrieta[15], P. Aubert[24], M. Backes[8], A. Balzer[9], M. Barnard[1], Y. Becherini[10], J. Becker Tjus[11], D. Berge[12], S. Bernhard[13], K. Bernlöhr[3], E. Birsin[7], R. Blackwell[14], M. Böttcher[1], C. Boisson[15], J. Bolmont[16], P. Bordas[3], J. Bregeon[17], F. Brun[18], P. Brun[18], M. Bryan[9], T. Bulik[19], M. Capasso[29], J. Carr[20], S. Casanova[21,3], N. Chakraborty[3], R. Chalme-Calvet[16], R. C. G. Chaves[17,22], A, Chen[23], J. Chevalier[24], M. Chrétien[16], S. Colafrancesco[23], G. Cologna[25], B. Condon[26], J. Conrad[27,⋆], C. Couturier[16], Y. Cui[28], I. D. Davids[1,8], B. Degrange[29], C. Deil[3], P. deWilt[14], A. Djannati-Ataï[30], W. Domainko[3], A. Donath[3], L. O'C. Drury[4], G. Dubus[31], K. Dutson[32], J. Dyks[33], M. Dyrda[21], T. Edwards[3], K. Egberts[34], P. Eger[3], J.-P. Ernenwein[20], S. Eschbach[35], C. Farnier[27,10], S. Fegan[29], M. V. Fernandes[2], A. Fiasson[24], G. Fontaine[29], A. Förster[3], S. Funk[35], M. Füßling[36], S. Gabici[30], M. Gajdus[7], Y. A. Gallant[17], T. Garrigoux[1], G. Giavitto[36], B. Giebels[29], J. F. Glicenstein[18], D. Gottschall[28], A. Goyal[37], M.-H. Grondin[26], M. Grudzińska[19], D. Hadasch[13], J. Hahn[3], J. Hawkes[14], G. Heinzelmann[2], G. Henri[31], G. Hermann[3], O. Hervet[15], A. Hillert[3], J. A. Hinton[3], W. Hofmann[3], C. Hoischen[34], M. Holler[29], D. Horns[2], A. Ivascenko[1], A. Jacholkowska[16], M. Jamrozy[37], M. Janiak[33], D. Jankowsky[35], F. Jankowsky[25], M. Jingo[23], T. Jogler[35], L. Jouvin[30], I. Jung-Richardt[35], M. A. Kastendieck[2], K. Katarzyński[38], U. Katz[35], D. Kerszberg[16], B. Khélifi[30], M. Kieffer[16], J. King[3], S. Klepser[36], D. Klochkov[28], W. Kluźniak[33], D. Kolitzus[13], Nu. Komin[23], K. Kosack[18], S. Krakau[11], M. Kraus[35], F. Krayzel[24], P. P. Krüger[1], H. Laffon[26], G. Lamanna[24], J. Lau[14], J.-P. Lees[24], J. Lefaucheur[30], V. Lefranc[18], A. Lemière[30], M. Lemoine-Goumard[26], J.-P. Lenain[16], E. Leser[34], T. Lohse[7], M. Lorentz[18], R. Liu[3], I. Lypova[36], V. Marandon[3], A. Marcowith[17], C. Mariaud[29], R. Marx[3], G. Maurin[24], N. Maxted[17], M. Mayer[7], P. J. Meintjes[39], U. Menzler[11], M. Meyer[27], A. M. W. Mitchell[3], R. Moderski[33], M. Mohamed[25], K. Morå[27], E. Moulin[18], T. Murach[7], M. de Naurois[29,⋆⋆], F. Niederwanger[13], J. Niemiec[21], L. Oakes[7], H. Odaka[3], S. Öttl[13], S. Ohm[36], M. Ostrowski[37], I. Oya[36], M. Padovani[17], M. Panter[3], R. D. Parsons[3], M. Paz Arribas[7], N. W. Pekeur[1], G. Pelletier[31], P.-O. Petrucci[31], B. Peyaud[18], S. Pita[30], H. Poon[3], D. Prokhorov[10], H. Prokoph[10], G. Pühlhofer[28], M. Punch[30,10], A. Quirrenbach[25], S. Raab[35], A. Reimer[13], O. Reimer[13], M. Renaud[17], R. de los Reyes[3], F. Rieger[3,40], C. Romoli[4], S. Rosier-Lees[24], G. Rowell[14,⋆⋆], B. Rudak[33], C. B. Rulten[15], V. Sahakian[6,5], D. Salek[41], D. A. Sanchez[24], A. Santangelo[28], M. Sasaki[28], R. Schlickeiser[11], F. Schüssler[18], A. Schulz[36], U. Schwanke[7], S. Schwemmer[25], A. S. Seyffert[1], N. Shafi[23], I. Shilon[35], R. Simoni[9], H. Sol[15], F. Spanier[1], G. Spengler[27], F. Spies[2], Ł. Stawarz[37], R. Steenkamp[8], C. Stegmann[34,36], F. Stinzing[35,†], K. Stycz[36], I. Sushch[1], J.-P. Tavernet[16], T. Tavernier[30], A. M. Taylor[4], R. Terrier[30], M. Tluczykont[2], C. Trichard[24], R. Tuffs[3], J. van der Walt[1], C. van Eldik[35], B. van Soelen[39], G. Vasileiadis[17], J. Veh[35], C. Venter[1], A. Viana[3], P. Vincent[16], J. Vink[9], F. Voisin[14], H. J. Völk[3], T. Vuillaume[24], Z. Wadiasingh[1], S. J. Wagner[25], P. Wagner[7], R. M. Wagner[27], R. White[3], A. Wierzcholska[21], P. Willmann[35], A. Wörnlein[35], D. Wouters[18], R. Yang[3], V. Zabalza[32], D. Zaborov[29], M. Zacharias[25], A. A. Zdziarski[33], A. Zech[15], F. Zefi[29], A. Ziegler[35], and N. Żywucka[37]

(Affiliations can be found after the references)

Received 12 April 2016 / Accepted 11 May 2016

ABSTRACT

Using the High Energy Spectroscopic System (H.E.S.S.) telescopes we have discovered a steady and extended very high-energy (VHE) γ-ray source towards the luminous blue variable candidate LBV 1806−20, massive stellar cluster Cl* 1806−20, and magnetar SGR 1806−20. The new VHE source, HESS J1808−204, was detected at a statistical significance of $>6\sigma$ (post-trial) with a photon flux normalisation $(2.9 \pm 0.4_{\rm stat} \pm 0.5_{\rm sys}) \times 10^{-13}$ ph cm^{-2} s^{-1} TeV^{-1} at 1 TeV and a power-law photon index of $2.3 \pm 0.2_{\rm stat} \pm 0.3_{\rm sys}$. The luminosity of this source (0.2 to 10 TeV; scaled to distance $d = 8.7$ kpc) is $L_{\rm VHE} \sim 1.6 \times 10^{34} (d/8.7\,{\rm kpc})^2$ erg s^{-1}. The VHE γ-ray emission is extended and is well fit by a single Gaussian with statistical standard deviation of $0.095° \pm 0.015°$. This extension is similar to that of the synchrotron radio nebula G10.0−0.3, which is thought to be powered by LBV 1806−20. The VHE γ-ray luminosity could be provided by the stellar wind luminosity of LBV 1806−20 by itself and/or the massive star members of Cl* 1806−20. Alternatively, magnetic dissipation (e.g. via reconnection) from SGR 1806−20 can potentially account for the VHE luminosity. The origin and hadronic and/or leptonic nature of the accelerated particles responsible for HESS J1808−204 is not yet clear. If associated with SGR 1806−20, the potentially young age of the magnetar (650 yr) can be used to infer the transport limits of these particles to match the VHE source size. This discovery provides new interest in the potential for high-energy particle acceleration from magnetars, massive stars, and/or stellar clusters.

Key words. gamma rays: general – stars: magnetars – stars: massive

1. Introduction

The magnetar SGR 1806−20 (e.g. Laros et al. 1986) is one of the most prominent and burst-active soft gamma repeaters (SGRs). It is best known for its giant flare of 27 December 2004 (Hurley et al. 2005), one of the strongest γ-ray outbursts recorded with a luminosity reaching $L \sim 10^{47}$ erg s^{-1} (from radio to hard X-ray energies). SGR 1806−20 is also a member of the massive stellar cluster Cl* 1806−20 (Fuchs et al. 1999; Eikenberry et al. 2001; Figer et al. 2005). This cluster harbours (within a 0.5′ radius) a number of energetic stars such as four Wolf-Rayet (WR) stars, five O-type stars, and a rare luminous blue variable candidate (cLBV), LBV 1806−20 (Kulkarni et al. 1995; van Kerkwijk et al. 1995).

⋆ Wallenberg Academy Fellow.
⋆⋆ Corresponding authors: H.E.S.S. Collaboration,
e-mail: contact.hess@hess-experiment.eu
† Deceased.

In addition to the giant flare, a number of less intense flares ($L \sim 10^{40}$–10^{43} erg s^{-1}) from SGR 1806−20 have also been seen in the past decade. The energy source for the flares is often attributed to magnetic torsion acting on and leading to deformation of the neutron star (NS) surface (Duncan & Thompson 1992; Paczynski 1992). The giant flare luminosity may instead result from accretion events onto a quark star (see e.g. Ouyed et al. 2007).

Magnetars are NSs with intense magnetic fields of order $B \sim 10^{14}$–10^{15} G. They represent one of nature's extreme astrophysical objects. Compared to canonical NSs (with $B \sim 10^{10}$ to 10^{13} G), magnetars exhibit slower spin rates (P of the order of a few seconds) but considerably faster spin-down rates ($\dot{P} \sim 10^{-11}$–10^{-9} s s^{-1}; see magnetar catalogue by Olausen & Kaspi 2014). For SGR 1806−20, the values $P = 7.6$ s and $\dot{P} = 7.5 \times 10^{-10}$ s s^{-1} have been determined (Nakagawa et al. 2009a), suggesting a spin-down power of $L_{\rm SD} \sim 10^{34}$–10^{35} erg s^{-1} (see also Mereghetti 2011 and Younes et al. 2015). This appears insufficient to account for the quiescent (unpulsed) X-ray emission with luminosity of $L_{\rm X} \sim 10^{35}$ erg s^{-1}.

The non-flaring X-ray emission is likely related to the decay of the intense magnetic field, which can theoretically yield a luminosity of $L_{\rm B} \sim 10^{35}$–10^{36} erg s^{-1} (Zhang 2003). This X-ray emission to which a variety of thermal and/or non-thermal models were fit is in fact variable and increased by a factor of 2 to 3 around the giant flare epoch of 2004/2005 (Mereghetti et al. 2007; Götz et al. 2007; Esposito et al. 2007; Nakagawa et al. 2009b). The quiescent X-ray emission is point-like as viewed by *Chandra* ($\lesssim 3''$), and a faint extension out to $\sim 1'$ due to scattering by dust (Kaplan et al. 2002; Svirski et al. 2011; Viganò et al. 2014) has been noticed in the two years following the giant flare of late 2004.

Interpretation of the $E < 10$ keV X-ray emission so far has centred on hot thermal gas with an additional non-thermal component arising from inverse-Compton (IC) scattering of NS thermal photons by NS wind electron/positron pairs. For $E > 10$ keV, the possibility of super-heated thermal Bremsstrahlung ($kT \sim 100$ keV), synchrotron, and IC emission has been debated (see reviews by Harding & Lai 2006 and Mereghetti 2011).

LBV 1806−20 may be one of the most luminous ($L > 5 \times 10^6 L_\odot$) and massive ($M \sim 100 M_\odot$) stars known (Eikenberry et al. 2004; Clark et al. 2005) although the possibility of a binary system has been suggested (Figer et al. 2004). The Cl* 1806−20 cluster age and combined stellar mass have been estimated at 3–4 Myr and >2000 $M_\odot$ respectively. However, SGR 1806−20 appears to be much younger with age ~650 yr (Tendulkar et al. 2012) based on proper motion of the magnetar and cluster member stars.

Given the high-mass loss rates associated with WR stars ($>10^{-5} M_\odot$ yr^{-1}) and the even higher rates for LBVs (e.g. Clark et al. 2005), the combined stellar wind kinetic energy in Cl* 1806−20 could reach $L_{\rm w} > 10^{38}$ erg s^{-1}. Cl* 1806−20 is enveloped in a synchrotron radio nebula (G10.0−0.3) with luminosity of $L_{\rm Rad} \sim 10^{32}$ erg s^{-1} (for $d = 8.7$ kpc, see below) extending over $\sim 9' \times 6'$ in size (Kulkarni et al. 1994). Originally linked to a supernova remnant (SNR), G10.0−0.3 is now believed to be powered by the intense stellar wind from LBV 1806−20 where the synchrotron flux of the nebula clearly peaks (Gaensler et al. 2001; Kaplan et al. 2002). The third source catalogue from *Fermi*-LAT (Acero et al. 2015) reports a confused[1] GeV γ-ray source, 3FGL J1809.2−2016c, towards the HII region G10.2−0.3 about 12′ to the Galactic north-west of Cl* 1806−20. G10.2−0.3 is a part of the giant HII complex W31 extending farther to the Galactic north (Corbel & Eikenberry 2004; see Fig. A.1). Distance estimates for Cl* 1806−20 are in a wide range of 6 to 19 kpc, based on a variety of techniques (Corbel & Eikenberry 2004; McClure-Griffiths & Gaensler 2005; Bibby et al. 2008; Svirski et al. 2011). We have adopted here the $8.7^{+1.8}_{-1.5}$ kpc distance from Bibby et al. (2008) who used stellar spectra and inferred luminosities of the Cl* 1806−20 cluster members.

Very high-energy (VHE) γ-ray emission has so far not been identified or associated with magnetars (Aleksić et al. 2013), despite the theoretical grounds for multi-TeV particle acceleration from or around them (Zhang et al. 2003; Arons 2003) with subsequent γ-ray and neutrino emission (e.g. Zhang et al. 2003; Ioka et al. 2005; Liu et al. 2010). Massive stars and clusters have been suggested as multi-GeV particle accelerators (e.g. Montmerle 1979; Voelk & Forman 1982; Eichler & Usov 1993; Domingo-Santamaría & Torres 2006; Bednarek 2007; Reimer et al. 2006) and several extended VHE γ-ray sources have been found towards them (Aharonian et al. 2002, 2007; Abramowski et al. 2012a). The high luminosities of SGR 1806−20, LBV 1806−20, and Cl* 1806−20, as well as the non-thermal radio, and hard X-ray emission seen towards these objects have motivated our search for VHE γ-ray emission with H.E.S.S.

2. H.E.S.S. VHE γ-ray observations, analysis, and results

VHE γ-ray observations have been carried out with the High Energy Stereoscopic System (H.E.S.S.) array of five imaging atmospheric Cherenkov telescopes (IACTs) located in the Khomas Highland of Namibia (16°30′00″ E 23°16′18″ S; 1800 m above sea level). The fifth telescope was added in 2012, but the data analysed here precede this installation, thus making use of the four original IACTs (with mirror area 107 m^2). These IACTs provide a stereoscopic view of extensive air showers (EAS) for reconstruction of γ-ray primary arrival direction and energy (Aharonian et al. 2006a). An event-by-event angular resolution of 0.06° (68% containment radius), energy resolution $\Delta E/E \lesssim 15\%$, and effective rejection of the background of cosmic-ray initiated EAS is achieved under a variety of analyses. An important feature of H.E.S.S. is its 5° field-of-view (FoV) diameter, which enables excellent survey coverage of the Galactic plane.

The SGR 1806−20/Cl* 1806−20 region was covered initially as part of the H.E.S.S. Galactic Plane Survey (HGPS; (Aharonian et al. 2006b), which commenced in 2004. Following the tentative indication of a signal, dedicated observation runs were carried out in 2009 and 2010. These runs used the so-called wobble mode (Aharonian et al. 2006a) in which the region of interest was offset by 0.7° from the telescope tracking positions to ensure adequate selection of reflected background regions in spectral analysis. After rejecting observation runs (which are typically 28 min in duration) based on the presence of clouds and instrumental problems, the total observation time towards SGR 1806−20 amounted to 94 h (from approximately 51 and 43 h of dedicated and HGPS data, respectively) after correcting for the H.E.S.S. off-axis response and readout dead time.

In this work we have employed the Model Analysis (de Naurois & Rolland 2009) (version `HESS_Soft_0-8-24`) in which the triggered Cherenkov images from the four 107 m^2

[1] Potentially contaminated by Galactic diffuse and/or strong neighbour source emission, especially at sub-GeV energies.

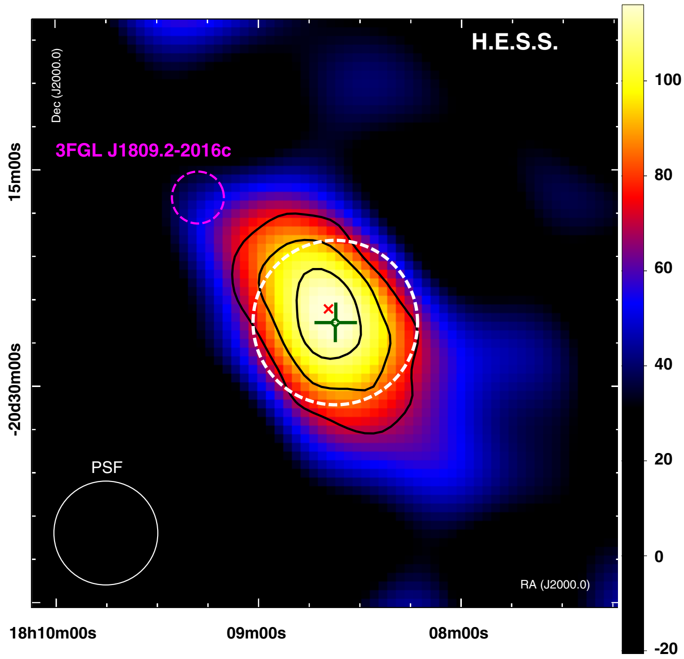

Fig. 1. H.E.S.S. exposure-corrected excess counts image of HESS J1808−204 towards the stellar cluster Cl* 1806−20 (red cross), containing SGR 1806−20 and LBV 1806−20. The image is Gaussian smoothed with standard deviation 0.06° corresponding to the 68% containment radius of the H.E.S.S. analysis PSF, which is also indicated by the white circle at the bottom left corner. Pre-trial excess significance contours (6, 5, 4σ levels) for an integration radius of 0.1° are indicated by black solid lines. The dark green solid point with error bars (1σ statistical) and white dashed ellipse represent the fitted location and radius of the intrinsic Gaussian source model. The 68% location error of 3FGL J1809.2−2016c (*Fermi*-LAT GeV source) is indicated by the magenta dashed ellipse.

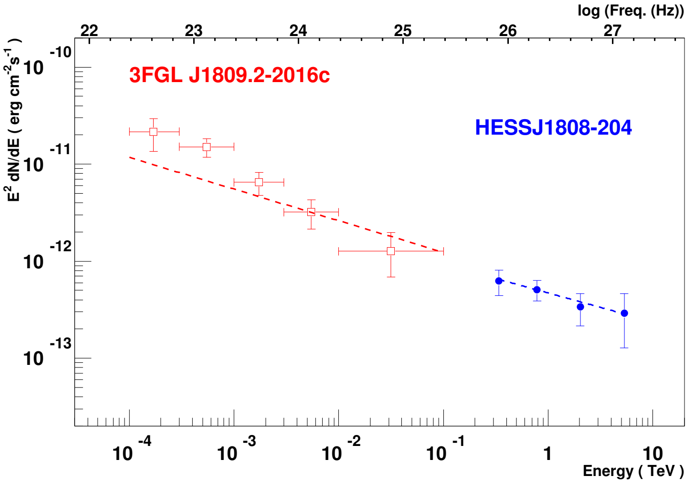

Fig. 2. Energy fluxes, 1σ statistical errors, and fitted pure power-law fits for HESS J1808−204 (blue solid points and blue dashed line) and the *Fermi*-LAT source 3FGL J1809.2−2016c (red open squares and red dashed line) from Acero et al. (2015).

IACTs are compared to a model image. Gamma-ray parameters such as arrival direction and energy are then extracted using a log-likelihood maximisation of the differences between the measured and modelled properties. The data were analysed using the faint cuts of the Model Analysis, which employs a minimum image size (total charge) of 120 photoelectrons for the Cherenkov images; similar results were obtained using standard cuts with a minimum charge of 60 photoelectrons. This analysis was used to generate detection statistics, images, energy spectra, and light curves, and has an energy threshold of $E > 0.15$ TeV for observations within 20° of the zenith. Averaged over all observations analysed here the threshold is ~0.4 TeV. Consistent results, within statistical and systematic errors, were obtained using alternate background methods such as the template background (Rowell 2003; Berge et al. 2007) and other analyses (Aharonian et al. 2006a; Becherini et al. 2011) that employed an independent event calibration procedure. Figure 1 presents the VHE γ-ray excess count image towards the Cl* 1806−20 region. The ring background model (Berge et al. 2007) was used to estimate the cosmic-ray background.

We found that a two-dimensional (2D) symmetrical Gaussian model describes well the intrinsic shape of the source with a 68% containment radius of 0.095° ± 0.015° (or 15 pc at 8.7 kpc distance). The fitted position, (J2000.0 epoch), is $\alpha = 18^{\rm h}08^{\rm m}37.3^{\rm s} \pm 5.1^{\rm s}_{\rm stat} \pm 1.3^{\rm s}_{\rm sys}$ and $\delta = -20°25'36.3'' \pm 71''_{\rm stat} \pm 20''_{\rm sys}$, with the systematic errors arising from telescope pointing and mechanical alignment uncertainties (see e.g. Aharonian et al. 2006a). Based on this we label the source HESS J1808−204. An asymmetric 2D Gaussian model (with major axis, minor axis, position angle anticlockwise from north) = (0.153° ± 0.029°, 0.058° ± 0.014°, 50.6° ± 7.8°) was also well fit to the intrinsic source shape. However, this model was only marginally preferred over a symmetric model (at the 2.4σ level), and so we defaulted to the symmetric model.

At the fitted position HESS J1808−204 has a pre-trial excess significance of +7.1σ and comprises 413 γ-ray photons within a radius of 0.2° (see Table A.1 for event statistics). This radius is a-priori-selected for extended source searching. After accounting for the 1600 trials in searching for this peak in a 0.4° × 0.4° region around SGR 1806−20 (40 × 40 bins), the post-trial significance is +6σ. Owing to the search binning oversampling the H.E.S.S. analysis point spread function (PSF), and the mixed nature of the data sets (Galactic plane scans and dedicated observations), we consider our post-trial significance to be conservative.

We calculated the photon spectrum from HESS J1808−204 centred on its fitted position with radius 0.2° to fully encompass the source. The reflected background model (Berge et al. 2007) was used to estimate the cosmic-ray background in each energy bin. Table A.2 summarises the photon fluxes and errors. The VHE γ-ray emission was well fit by a power law ($dN/dE = \phi(E/{\rm TeV})^{-\Gamma}$) with parameters $\phi = (2.9 \pm 0.4_{\rm stat} \pm 0.5_{\rm sys}) \times 10^{-13}$ ph cm^{-2} s^{-1} TeV^{-1} and $\Gamma = 2.3 \pm 0.2_{\rm stat} \pm 0.3_{\rm sys}$ (probability = 0.4). The VHE spectral fluxes and power-law fits, and also those of 3FGL J1809.2−2016c, are shown in Fig. 2 for comparison.

Since an additional variable VHE γ-ray emission component could be expected from SGR 1806−20 and possibly from the member stars of Cl* 1806−20, we examined the flux light curve ($\phi > 1$ TeV) for a point-like test region of radius 0.1°, which is optimal for the H.E.S.S. analysis PSF, encompassing these objects over nightly and lunar monthly (dark lunar periods) timescales (see Fig. 3). We found that the >1 TeV flux light curve was well fit by a steady flux level with $\chi^2/\nu = 80.6/88$ for nightly and $\chi^2/\nu = 15.2/12$ for lunar monthly timescales, respectively, indicating no evidence for variability in the VHE γ-ray emission towards SGR 1806−20 and/or Cl* 1806−20. A number of soft-γ-ray flares of SGR 1806−20 occurred since our observations commenced, including the giant flare of 27 December 2004, and several other intermediate flares of note (based on announcements from the Gamma-Ray Coordinates Network).

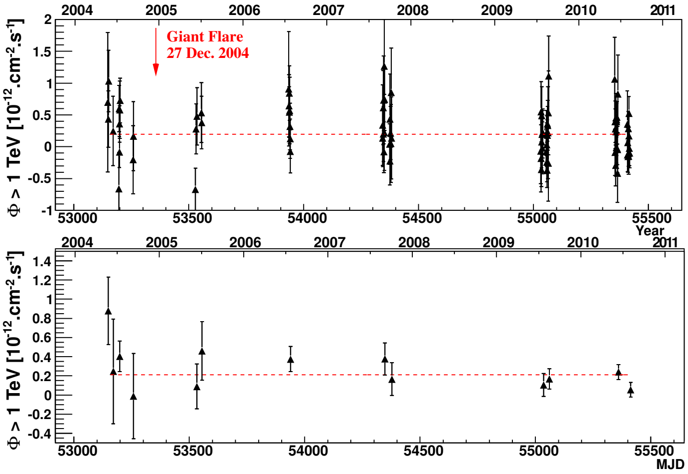

Fig. 3. Light curve of the nightly (*top*) and lunar monthly (*bottom*) VHE γ-ray emission ($\phi > 1$ TeV) from a point-like source (integration radius 0.1°) centred on SGR 1806−20. The red dashed line indicates the average flux level in each case and giant flare of 27 December 2004 is indicated on the nightly light curve.

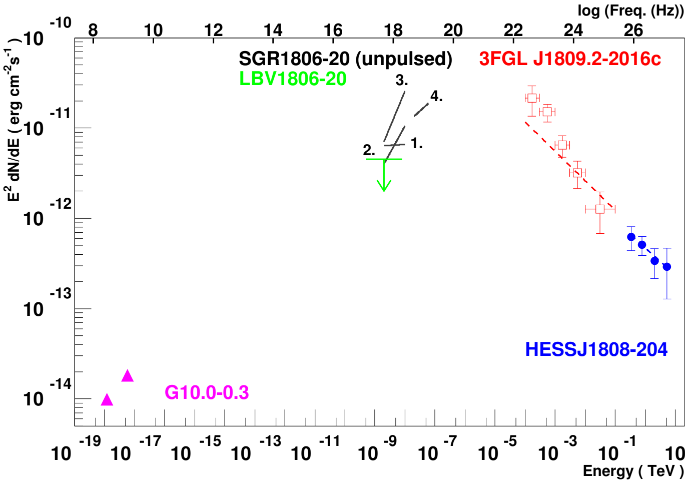

Fig. 4. Energy flux (1σ statistical error bars) for HESS J1801−204 and multiwavelength comparisons. Included is the *Fermi*-LAT GeV emission (Acero et al. 2015), VLA radio emission for G10.0−0.3 (Kulkarni et al. 1994), SGR 1806−20 X-ray unpulsed emission (power-law fits: 1. *Beppo*-SAX 21 Mar. 1999; 2. *XMM-Newton* 3 Apr. 2002; 3. *XMM-Newton* 6 Oct. 2004; and 4. INTEGRAL IBIS 2006/2007 from Esposito et al. 2007), and X-ray upper limit for LBV 1806−20 (Nazé et al. 2012).

Our first two periods of H.E.S.S. observations were taken several months on either side of the giant flare. We note that the extent of the H.E.S.S. analysis PSF could integrate steady VHE γ-ray emission from several sources in the region, diluting any possible variable or periodic emission from a single source such as SGR 1806−20. Additionally, the highly variable spin-down rate $\dot{P}$ of SGR 1806−20 (Woods et al. 2007; Mereghetti 2011; Viganò et al. 2014; Younes et al. 2015) over the past decade and infrequently sampled ephemeris (from X-ray measurements) further complicate the search for any pulsed VHE detection. We leave such a study to further work.

3. Discussion

Potential counterparts to the VHE γ-ray source HESS J1808−204 are the magnetar SGR 1806−20, the massive stellar cluster Cl* 1806−20, and/or energetic member stars of the cluster, in particular LBV 1806−20 and/or the WR stars. HESS J1808−204 exhibits an energy flux (0.2 to 10 TeV) of $F_{\rm VHE} \sim 1.7 \times 10^{-12}$ erg cm^{-2} s^{-1} and luminosity of $L_{\rm VHE} \sim 1.6 \times 10^{34}$ $(d/8.7\,{\rm kpc})^2$ erg s^{-1}. Figure 4 presents the energy fluxes of the VHE and multiwavelength sources in this region (highlighting the prominence of the γ-ray emission), including an X-ray upper limit for LBV 1806−20 (Nazé et al. 2012). There are no signs of any SNRs (although one should exist to explain SGR 1806−20) or other energetic pulsars in the region. However, a prominent multiwavelength feature is the synchrotron radio nebula G10.0−0.3. Interestingly, HESS J1808−204 is very similar in intrinsic size to G10.0−0.3 as shown in Fig. 5. Based on this, LBV 1806−20 (the possible source of energy for G10.0−0.3) could be considered a plausible counterpart.

With a likely kinetic stellar wind luminosity of $L_{\rm W} > 10^{38}$ erg s^{-1}, the cluster Cl* 1806−20 could easily account for the VHE γ-ray luminosity of HESS J1808−204 and also of the nearby *Fermi*-LAT source. Of the member stars, the four WR stars and in particular LBV 1806−20 could dominate this stellar wind energy and therefore drive much of the particle acceleration. The VHE γ-ray emission would represent only a small fraction $\sim 10^{-4}$ of the cLBV's wind luminosity, $L_{\rm LBV} \sim 10^{38}$ erg s^{-1}, for example.

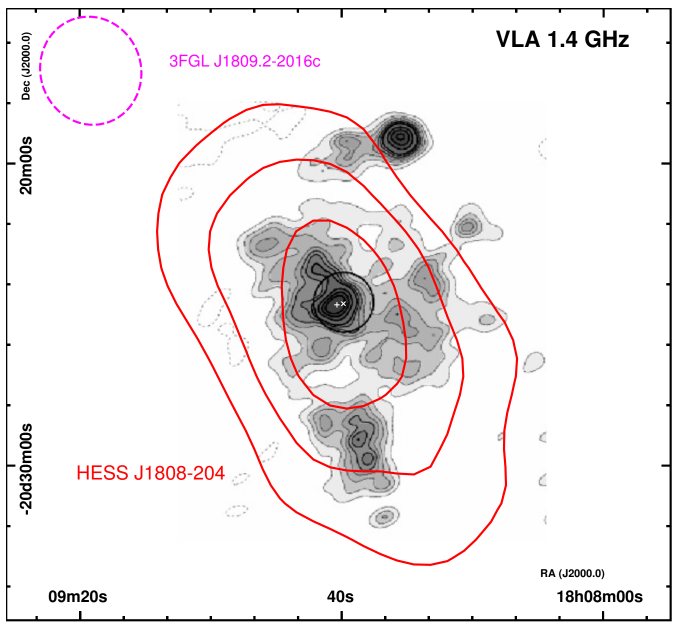

Fig. 5. VLA 1.4 GHz radio image of the radio nebula G10.0−0.3 (contour levels at −3, 2, 4, 6, 8, 10, 12, 14, 20, 25, 30×1.56 mJy/beam; black circle indicating an ASCA X-ray source location) from Kulkarni et al. (1994) with red solid VHE γ-ray contours of HESS J1808−204 (as per Fig. 1). The 68% location error of 3FGL J1809.2−2016c is indicated by the magenta dashed ellipse, and locations of SGR 1806−20 (x) and LBV 1806−20 (+) are indicated.

In a scenario involving the cluster of massive stars, particle acceleration could take place as a result of the stellar wind interaction over parsec scales according to the cluster size and stellar density. Several extended VHE γ-ray sources have already been linked to such processes likely to be present in massive stellar clusters (e.g. in Cyg OB2, Westerlund 2 and Westerlund 1; Aharonian et al. 2002, 2007; Abramowski et al. 2012a). Here, Westerlund 1 may bear some resemblance to Cl* 1806−20 as it also harbours a magnetar (the anomalous X-ray pulsar

CXOU J164710.2−455216; Muno et al. 2007) and a LBV star (Wd1-243; see e.g. Clark et al. 2008). A point of difference is that the VHE emission towards Westerlund 1 is physically about a factor 10 larger than that towards Cl* 1806−20 (radii of 160 pc vs. 15 pc).

The luminosity of LBV 1806−20, $L \sim 10^{6.3}\ L_{\odot}$, ranks it in the top five amongst the 35 LBV and cLBV list (Clark et al. 2005) (see Kniazev et al. 2015 for the most recent catalogue of LBVs). VHE γ-ray emission is found towards four of the top five in this list: the Pistol-Star and FMM 362 towards the diffuse VHE Galactic centre emission (Aharonian et al. 2006c), Cyg OB2#12 towards TeV J2032+4130 (Aharonian et al. 2002), and Wray 17-96 in the vicinity of HESS J1741−302 (Tibolla et al. 2009). It remains to be seen, however, how these LBVs are related to their nearby VHE γ-ray sources. The notable exception is η-Car, which is probably the most luminous LBV. η-Car exhibits γ-ray emission (up to about 200 GeV) modulated by its orbital period of 5.54 yr (?Abdo et al. 2010; Tavani et al. 2009; Reitberger et al. 2015), suggesting a wind-wind interaction as the source of particle acceleration. A similar process may be active in LBV 1806−20 since it too may be a binary system.

The linkage between HESS J1808−204 and the *Fermi*-LAT GeV source 3FGL J1809.2−2016c is not so clear given the significant spatial separation between the two and the confused nature of the GeV source. For confused GeV sources there are considerable systematic uncertainties in location and existence above the diffuse GeV background. As a result, the sub-GeV spectral determination is usually compromised (as is readily apparent in Figs. 2 and 4). Thus, even though the fitted power -law index of the GeV source ($\Gamma_{\rm GeV} = 2.33 \pm 0.09$ from Acero et al. 2015) is very similar to that of HESS J1808−204, and its extrapolation to TeV energies is within systematic errors that are consistent with the VHE flux points, the above-mentioned caveats prevent further detailed comparisons. In the case in which the GeV and VHE sources are nevertheless connected via the same putative particle accelerator, the γ-ray luminosity would increase by about a factor of 5 to 10 to account for the dominant GeV component ($L_{\rm GeV} \sim 10^{35}$ erg s^{-1} at 8.7 kpc).

Turning our attention to SGR 1806−20, the VHE γ-ray luminosity is up to ~50% of this magnetar's spin-down power. The established VHE pulsar wind nebulae (PWN) have VHE spin-down efficiencies of $L_{\rm VHE}/L_{\rm SD} \lesssim 10\%$ and are associated with pulsars exhibiting high spin-down power of $L_{\rm SD} > 10^{35}$ erg s^{-1} (Halpern & Gotthelf 2010), in contrast to the situation here. The quiescent X-ray luminosity for SGR 1806−20 is also similar to or greater than its spin-down power, suggesting the X-rays result from magnetic energy perhaps via reconnection (Zhang 2003) rather than the rotational energy associated with pulsar spin-down. The luminosity of the nearby *Fermi*-LAT GeV source could also be met by magnetic energy. Moreover, the rather low ratio $L_{\rm VHE}/L_{\rm X} \sim 0.1$ (for the X-ray luminosity $L_{\rm X}$ in the 2 to 10 keV range) is clearly at odds with the observed trend of $L_{\rm VHE}/L_{\rm X} \gtrsim 10$ for pulsars with $L_{\rm SD} < 10^{36}$ erg s^{-1} (Mattana et al. 2009). Hence if HESS J1808−240 is attributed to electrons accelerated by SGR 1806−20, it is likely that magnetic energy is the source of power.

Given the presence of several molecular clouds along the line of sight towards Cl* 1806−20 (Corbel & Eikenberry 2004), a hadronic origin for HESS J1808−204 involving collisions of multi-TeV protons with interstellar gas is worth considering. The singly pointed CO observations of Corbel & Eikenberry (2004) however do not reveal the spatial distribution, mass, or density of the molecular clouds. Studies of the molecular cloud morphology are hence needed to ascertain the detailed likelihood of a hadronic origin for the HESS J1808−204 and the transport properties of particles from the Cl* 1806−20 region. Nevertheless based on the integrated CO brightness temperatures reported in Table 2 of Corbel & Eikenberry (2004), we estimated approximate proton densities n of the order of 10^3 cm^{-3} for the brighter clouds MC 13A, MC 73, and MC 44 (as labelled by Corbel & Eikenberry 2004) at their respective distances when integrating over the 45″ beam full width at half maximum (FWHM) of the telescope used in the CO observations (Corbel & Eikenberry 2004 favoured MC 13A as most likely associated with the cluster). These densities may be considered upper limits to the wider cloud densities since the CO measurements were taken towards the stellar cluster where molecular gas density may be expected to peak.

Using the relation $B \sim 10(n\,/\,300\ {\rm cm}^{-3})^{0.65}\ \mu$G from Crutcher et al. (2010), magnetic fields of order $B \sim 20\ \mu$G could be expected inside the clouds. From here and assuming a turbulent B-field, we can employ the formalism of Gabici et al. (2007) (Eq. (2)) for the diffusion coefficient as a function of magnetic field B and suppression factor χ, which is used to account for increased magnetic field turbulence related to cosmic-ray streaming instabilities in the interstellar medium. We note however that the cosmic-ray transport may not necessarily be diffusive in the case of a more ordered B-field structure, as for example indicated by Crutcher et al. (2010) in molecular clouds of low density $n < 300$ cm^{-3}. We can, nevertheless, use the young age (650 years) of SGR 1806−20 to provide some limits on the diffusion distances of particles. For 50 TeV protons coming from the magnetar and assuming $\chi = 1$, we arrive at a diffusion length of $l \sim 30$ pc, which is approaching the observed ~15 pc radius of HESS J1808−204. The parameter χ is poorly constrained, but Protheroe et al. (2008) have suggested $\chi < 0.01$−0.1 based on observations of the GeV γ-ray emission towards the dense Sgr B2 giant molecular cloud.

We can also infer the cosmic-ray proton energy budget $W_p = L_{\rm VHE}({\rm erg\ s^{-1}})\tau_{\rm pp}$ erg required to power HESS J1808−204. Here, $\tau_{\rm pp} \sim 1.7\times10^{15}/n$ cm^{-3} s is the cooling time for γ-rays produced by proton-proton collisions as a function of the target density n. For the density discussed above we find $W_p \sim 10^{46}$ erg. This is rather modest compared to that of a canonical supernova remnant, however, our estimate for W_p would be a lower limit since the density is likely an upper limit as explained above.

An alternative, leptonic origin for HESS J1808−204 might arise from IC scattering of local soft photon fields by TeV to multi-TeV electrons. The local infrared (IR) field (due to heated dust) peaks strongly towards Cl* 1806−20 (Rahoui et al. 2009) with an energy density of ~20 to 50 eV cm^{-3} as measured by *Spitzer* at 24 μm within ~30″ of Cl* 1806−20 (see Fig. A.1). Measured over the 15 pc radius of VHE γ-ray emission region, however, the IR energy density, ~0.4 eV cm^{-3}, is comparable to that of the cosmic microwave background (CMB) at 0.25 eV cm^{-3}. An additional soft photon field comes from the optical/UV photons from the massive stellar content of Cl* 1806−20. Based on the presence of five OB, four WR stars, and one cLBV (Figer et al. 2005; Edwards et al. 2011), we estimated a bolometric luminosity of ~10^{40} erg s^{-1}. Averaged over the VHE γ-ray emission region, the resulting optical/UV energy density is ~7 eV cm^{-3}.

Considering the TeV to multi-TeV electron energy loss rate for IC scattering taking into account Klein-Nishina effects (e.g. Eq. (35) of Aharonian & Atoyan 1981) with these energy densities, we find that the dominant IC component will likely come from up-scattered CMB photons in the Thomson scattering regime as the Klein-Nishina effect will suppress the IR and optical/UV components. Thus we can take the X-ray power-law components of SGR 1806−20 ($F_X \sim$ few $\times 10^{-11}$ erg s^{-1} cm^{-2}) as synchrotron emission from multi-TeV electrons and the VHE γ-ray flux $F_{\rm VHE}$ as arising from IC scattering of the CMB photons by the same electrons. From consideration of the IC and synchrotron luminosities, assuming IC emission only comes from up-scattered CMB photons in the Thomson regime, the magnetic field $B \sim 10\sqrt{\xi F_X/(10 F_{\rm VHE})}\,\mu$G in the region common to both fluxes can be estimated. Here the factor ξ accounts for the radii of the VHE and X-ray emission ($\xi = (R_{\rm VHE}/R_X)^2$).

We estimate $B \gtrsim 1$ mG for the values $R_{\rm VHE} \sim 360''$ (VHE radius) and $R_X \lesssim 3''$ (Kaplan et al. 2002), which might be expected given the extreme magnetic field of SGR 1806−20 and that of the massive stars in Cl* 1806−20. The sub-parsec size of the X-ray emission region (Kaplan et al. 2002) is also consistent with a magnetic field $B \sim$ few mG if the synchrotron cooling time ($t_{\rm sync} <$ few yr) dominantly limits the transport of the parent multi-TeV electrons. There are in fact a number of other high magnetic field pulsars with compact X-ray nebulae potentially associated with unidentified VHE γ-ray sources (e.g. see Kargaltsev et al. 2013) that may be explained within this scenario.

The 15 pc radius of the TeV emission region could be allowed by the much longer IC cooling time of $t_{\rm IC} \sim 10^3$–10^4 yr, provided that the magnetic field has declined to $\lesssim$10 μG outside the X-ray region to avoid synchrotron losses. A reduced B field is in fact implied by the X-ray upper limit (4.53×10^{-12} erg s^{-1} cm^{-2}) for LBV 1806−20 (Nazé et al. 2012), and is only 15″ away from SGR 1806−20. Such a reduction in the B-field may also play a role in limiting the X-ray emission region size around SGR 1806−20, by permitting electrons to escape to the wider IC-dominated region; the electron diffusion coefficient would likely increase as well, further enhancing their escape. Our inferred B-field value of ∼20 μG from the molecular cloud column density as discussed earlier, may still limit the level of IC emission. As argued earlier for the hadronic interpretation, however, spatial studies of the molecular gas will be needed to more confidently discriminate hadronic and leptonic models for HESS J1808−204.

4. Conclusions

We report the discovery with the H.E.S.S. telescopes of extended VHE γ-ray emission (HESS J1808−204) towards the luminous blue variable candidate LBV 1806−20, the massive stellar cluster Cl* 1806−20, and the magnetar SGR 1806−20. The H.E.S.S. telescopes are not able to resolve these potential counterparts, which are located within a 0.5′ radius. However the extension of the γ-ray emission, at ∼0.1° radius (or 15 pc for a distance of 8.7 kpc) is similar in scale to the radio nebula G10.0−0.3 supposedly powered by LBV 1806−20. The intense stellar wind luminosity of LBV 1806−20, by itself or collectively from the other massive stars in Cl* 1806−20, could readily power the VHE source, which has a luminosity of $L_{\rm VHE} \sim 1.6 \times 10^{34} (d/8.7\,{\rm kpc})^2$ erg s^{-1}. If associated with SGR 1806−20, the reported young age of 650 yr for this magnetar, along with our estimated magnetic field of 20 μG, could imply a diffusive transport limit of <30 pc which is similar to the size of the VHE emission. Additionally, in this case the VHE luminosity could only realistically be met by magnetic dissipative effects rather than the magnetar spin-down process. Whatever the origin of the parent particles responsible for HESS J1804−204, their hadronic and/or leptonic nature is currently unclear. Detailed observations of the molecular gas spatial distribution would be needed for some discrimination of hadronic from leptonic scenarios (in particular by providing constraints on the magnetic field in the region). Looking towards the future, the arc-minute angular resolution of the forthcoming Cherenkov Telescope Array (Acharya et al. 2013) will be able to probe the VHE morphology on the parsec scales necessary to probe for energy dependent morphology, providing further information about the nature and origin of the particles responsible for HESS J1804−204. In summary, the discovery of HESS J1808−204 provides further impetus to the notion that magnetars, massive stars, and/or stellar clusters can accelerate particles to beyond TeV energies.

Acknowledgements. The support of the Namibian authorities and of the University of Namibia in facilitating the construction and operation of H.E.S.S. is gratefully acknowledged, as is the support by the German Ministry for Education and Research (BMBF), the Max Planck Society, the German Research Foundation (DFG), the French Ministry for Research, the CNRS-IN2P3 and the Astroparticle Interdisciplinary Programme of the CNRS, the UK Science and Technology Facilities Council (STFC), the IPNP of the Charles University, the Czech Science Foundation, the Polish Ministry of Science and Higher Education, the South African Department of Science and Technology and National Research Foundation, the Australian Research Council and by the University of Namibia. We appreciate the excellent work of the technical support staff in Berlin, Durham, Hamburg, Heidelberg, Palaiseau, Paris, Saclay, and in Namibia in the construction and operation of the equipment.

References

Abdo, A. A., Ackermann, M., Ajello, M., et al. 2010, ApJ, 723, 649
Abramowski, A., Acero, F., Aharonian, F., et al. 2012a, A&A, 537, A114
Abramowski, A., Acero, F., Aharonian, F., et al. 2012b, MNRAS, 424, 128
Acero, F., Ackermann, M., Ajello, M., et al. 2015, ApJS, 218, 23
Acharya, B. S., Actis, M., Aghajani, T., et al. 2013, Astropart. Phys., 43, 3
Aharonian, F. A., & Atoyan, A. M. 1981, Ap&SS, 79, 321
Aharonian, F., Akhperjanian, A., Beilicke, M., et al. 2002, A&A, 393, L37
Aharonian, F., Akhperjanian, A. G., Bazer-Bachi, A. R., et al. 2006a, A&A, 457, 899
Aharonian, F., Akhperjanian, A. G., Bazer-Bachi, A. R., et al. 2006b, ApJ, 636, 777
Aharonian, F., Akhperjanian, A. G., Bazer-Bachi, A. R., et al. 2006c, Nature, 439, 695
Aharonian, F., Akhperjanian, A. G., Bazer-Bachi, A. R., et al. 2007, A&A, 467, 1075
Aleksić, J., Antonelli, L. A., Antoranz, P., et al. 2013, A&A, 549, A23
Arons, J. 2003, ApJ, 589, 871
Becherini, Y., Djannati-Ataï, A., Marandon, V., Punch, M., & Pita, S. 2011, Astropart. Phys., 34, 858
Bednarek, W. 2007, MNRAS, 382, 367
Berge, D., Funk, S., & Hinton, J. 2007, A&A, 466, 1219
Bibby, J. L., Crowther, P. A., Furness, J. P., & Clark, J. S. 2008, MNRAS, 386, L23
Clark, J. S., Larionov, V. M., & Arkharov, A. 2005, A&A, 435, 239
Clark, J. S., Muno, M. P., Negueruela, I., et al. 2008, A&A, 477, 147
Corbel, S., & Eikenberry, S. S. 2004, A&A, 419, 191
Crutcher, R. M., Wandelt, B., Heiles, C., Falgarone, E., & Troland, T. H. 2010, ApJ, 725, 466
de Naurois, M., & Rolland, L. 2009, Astropart. Phys., 32, 231
Domingo-Santamaría, E., & Torres, D. F. 2006, A&A, 448, 613
Duncan, R. C., & Thompson, C. 1992, ApJ, 392, L9
Edwards, M. L., Bandyopadhyay, R. M., Eikenberry, S. S., Mikles, V. J., & Moon, D.-S. 2011, in IAU Symp. 272, eds. C. Neiner, G. Wade, G. Meynet, & G. Peters, 606
Eichler, D., & Usov, V. 1993, ApJ, 402, 271
Eikenberry, S. S., Garske, M. A., Hu, D., et al. 2001, ApJ, 563, L133
Eikenberry, S. S., Matthews, K., LaVine, J. L., et al. 2004, ApJ, 616, 506
Esposito, P., Mereghetti, S., Tiengo, A., et al. 2007, A&A, 476, 321
Figer, D. F., Najarro, F., & Kudritzki, R. P. 2004, ApJ, 610, L109
Figer, D. F., Najarro, F., Geballe, T. R., Blum, R. D., & Kudritzki, R. P. 2005, ApJ, 622, L49
Fuchs, Y., Mirabel, F., Chaty, S., et al. 1999, A&A, 350, 891
Gabici, S., Aharonian, F. A., & Blasi, P. 2007, Ap&SS, 309, 365
Gaensler, B. M., Slane, P. O., Gotthelf, E. V., & Vasisht, G. 2001, ApJ, 559, 963
Götz, D., Mereghetti, S., & Hurley, K. 2007, Ap&SS, 308, 51

Halpern, J. P., & Gotthelf, E. V. 2010, ApJ, 725, 1384
Harding, A. K., & Lai, D. 2006, Rep. Prog. Phys., 69, 2631
Hurley, K., Boggs, S. E., Smith, D. M., et al. 2005, Nature, 434, 1098
Ioka, K., Razzaque, S., Kobayashi, S., & Mészáros, P. 2005, ApJ, 633, 1013
Kaplan, D. L., Fox, D. W., Kulkarni, S. R., et al. 2002, ApJ, 564, 935
Kargaltsev, O., Rangelov, B., & Pavlov, G. 2013, in The Universe Evolution: Astrophysical and Nuclear Aspects, eds. I. Strakovsky, & L. Blokhintsev (Nova Science Publ.), 359
Kniazev, A. Y., Gvaramadze, V. V., & Berdnikov, L. N. 2015, MNRAS, 449, L60
Kulkarni, S. R., Frail, D. A., Kassim, N. E., Murakami, T., & Vasisht, G. 1994, Nature, 368, 129
Kulkarni, S. R., Matthews, K., Neugebauer, G., et al. 1995, ApJ, 440, L61
Laros, J. G., Fenimore, E. E., Fikani, M. M., Klebesadel, R. W., & Barat, C. 1986, Nature, 322, 152
Li, T.-P., & Ma, Y.-Q. 1983, ApJ, 272, 317
Liu, X.-W., Wu, X.-F., & Lu, T. 2010, New Astron., 15, 292
Mattana, F., Falanga, M., Götz, D., et al. 2009, ApJ, 694, 12
McClure-Griffiths, N. M., & Gaensler, B. M. 2005, ApJ, 630, L161
Mereghetti, S. 2011, Adv. Space Res., 47, 1317
Mereghetti, S., Esposito, P., & Tiengo, A. 2007, Ap&SS, 308, 13
Montmerle, T. 1979, ApJ, 231, 95
Muno, M. P., Gaensler, B. M., Clark, J. S., et al. 2007, MNRAS, 378, L44
Nakagawa, Y. E., Mihara, T., Yoshida, A., et al. 2009a, PASJ, 61, 387
Nakagawa, Y. E., Yoshida, A., Yamaoka, K., & Shibazaki, N. 2009b, PASJ, 61, 109
Nazé, Y., Rauw, G., & Hutsemékers, D. 2012, A&A, 538, A47
Olausen, S. A., & Kaspi, V. M. 2014, ApJS, 212, 6
Ouyed, R., Leahy, D., & Niebergal, B. 2007, A&A, 473, 357
Paczynski, B. 1992, Acta Astron., 42, 145
Protheroe, R. J., Ott, J., Ekers, R. D., Jones, D. I., & Crocker, R. M. 2008, MNRAS, 390, 683
Rahoui, F., Chaty, S., & Lagage, P.-O. 2009, A&A, 493, 119
Reimer, A., Pohl, M., & Reimer, O. 2006, ApJ, 644, 1118
Reitberger, K., Reimer, A., Reimer, O., & Takahashi, H. 2015, A&A, 577, A100
Rowell, G. P. 2003, A&A, 410, 389
Svirski, G., Nakar, E., & Ofek, E. O. 2011, MNRAS, 415, 2485
Tavani, M., Sabatini, S., Pian, E., et al. 2009, ApJ, 698, L142
Tendulkar, S. P., Cameron, P. B., & Kulkarni, S. R. 2012, ApJ, 761, 76
Tibolla, O., Komin, N., Kosack, K., & Naumann-Godo, M. 2009, in AIP Conf. Ser., 1112, 233
van Kerkwijk, M. H., Kulkarni, S. R., Matthews, K., & Neugebauer, G. 1995, ApJ, 444, L33
Viganò, D., Rea, N., Esposito, P., et al. 2014, J. High Energy Astrophysics, 3, 41
Voelk, H. J., & Forman, M. 1982, ApJ, 253, 188
Woods, P. M., Kouveliotou, C., Finger, M. H., et al. 2007, ApJ, 654, 470
Younes, G., Kouveliotou, C., & Kaspi, V. M. 2015, ApJ, 809, 165
Zhang, B. 2003, in Proc. Int. Workshop on Strong Magnetic Fields and Neutron Star, 83
Zhang, B., Dai, Z. G., Mészáros, P., Waxman, E., & Harding, A. K. 2003, ApJ, 595, 346

[1] Centre for Space Research, North-West University, 2520 Potchefstroom, South Africa
[2] Universität Hamburg, Institut für Experimentalphysik, Luruper Chaussee 149, 22761 Hamburg, Germany
[3] Max-Planck-Institut für Kernphysik, PO Box 103980, 69029 Heidelberg, Germany
[4] Dublin Institute for Advanced Studies, 31 Fitzwilliam Place, Dublin 2, Ireland
[5] National Academy of Sciences of the Republic of Armenia, Marshall Baghramian Avenue, 24, 0019 Yerevan, Republic of Armenia
[6] Yerevan Physics Institute, 2 Alikhanian Brothers St., 375036 Yerevan, Armenia
[7] Institut für Physik, Humboldt-Universität zu Berlin, Newtonstr. 15, 12489 Berlin, Germany
[8] University of Namibia, Department of Physics, 13301 Private Bag, Windhoek, Namibia
[9] GRAPPA, Anton Pannekoek Institute for Astronomy, University of Amsterdam, Science Park 904, 1098 XH Amsterdam, The Netherlands
[10] Department of Physics and Electrical Engineering, Linnaeus University, 351 95 Växjö, Sweden
[11] Institut für Theoretische Physik, Lehrstuhl IV: Weltraum und Astrophysik, Ruhr-Universität Bochum, 44780 Bochum, Germany
[12] GRAPPA, Anton Pannekoek Institute for Astronomy and Institute of High-Energy Physics, University of Amsterdam, Science Park 904, 1098 XH Amsterdam, The Netherlands
[13] Institut für Astro- und Teilchenphysik, Leopold-Franzens-Universität Innsbruck, 6020 Innsbruck, Austria
[14] School of Chemistry & Physics, University of Adelaide, 5005 Adelaide, Australia
[15] LUTH, Observatoire de Paris, PSL Research University, CNRS, Université Paris Diderot, 5 Place Jules Janssen, 92190 Meudon, France
[16] Sorbonne Universités, UPMC Université Paris 06, Université Paris Diderot, Sorbonne Paris Cité, CNRS, Laboratoire de Physique Nucléaire et de Hautes Energies (LPNHE), 4 place Jussieu, 75252 Paris Cedex 5, France
[17] Laboratoire Univers et Particules de Montpellier, Université Montpellier, CNRS/IN2P3, CC 72, Place Eugène Bataillon, 34095 Montpellier Cedex 5, France
[18] DSM/Irfu, CEA Saclay, 91191 Gif-Sur-Yvette Cedex, France
[19] Astronomical Observatory, The University of Warsaw, Al. Ujazdowskie 4, 00-478 Warsaw, Poland
[20] Aix Marseille Université, CNRS/IN2P3, CPPM UMR 7346, 13288 Marseille, France
[21] Instytut Fizyki Jądrowej PAN, ul. Radzikowskiego 152, 31-342 Kraków, Poland
[22] Funded by EU FP7 Marie Curie, grant agreement No. PIEF-GA-2012-332350,
[23] School of Physics, University of the Witwatersrand, 1 Jan Smuts Avenue, Braamfontein, 2050 Johannesburg, South Africa
[24] Laboratoire d'Annecy-le-Vieux de Physique des Particules, Université Savoie Mont-Blanc, CNRS/IN2P3, 74941 Annecy-le-Vieux, France
[25] Landessternwarte, Universität Heidelberg, Königstuhl, 69117 Heidelberg, Germany
[26] Université Bordeaux, CNRS/IN2P3, Centre d'Études Nucléaires de Bordeaux Gradignan, 33175 Gradignan, France
[27] Oskar Klein Centre, Department of Physics, Stockholm University, Albanova University Center, 10691 Stockholm, Sweden
[28] Institut für Astronomie und Astrophysik, Universität Tübingen, Sand 1, 72076 Tübingen, Germany
[29] Laboratoire Leprince-Ringuet, Ecole Polytechnique, CNRS/IN2P3, 91128 Palaiseau, France
[30] APC, AstroParticule et Cosmologie, Université Paris Diderot, CNRS/IN2P3, CEA/Irfu, Observatoire de Paris, Sorbonne Paris Cité, 10 rue Alice Domon et Léonie Duquet, 75205 Paris Cedex 13, France
[31] Univ. Grenoble Alpes, IPAG, CNRS, IPAG, 38000 Grenoble, France
[32] Department of Physics and Astronomy, The University of Leicester, University Road, Leicester, LE1 7RH, UK
[33] Nicolaus Copernicus Astronomical Center, ul. Bartycka 18, 00-716 Warsaw, Poland
[34] Institut für Physik und Astronomie, Universität Potsdam, Karl-Liebknecht-Strasse 24/25, 14476 Potsdam, Germany
[35] Universität Erlangen-Nürnberg, Physikalisches Institut, Erwin-Rommel-Str. 1, 91058 Erlangen, Germany
[36] DESY, 15738 Zeuthen, Germany
[37] Obserwatorium Astronomiczne, Uniwersytet Jagielloński, ul. Orla 171, 30-244 Kraków, Poland
[38] Centre for Astronomy, Faculty of Physics, Astronomy and Informatics, Nicolaus Copernicus University, Grudziadzka 5, 87-100 Torun, Poland
[39] Department of Physics, University of the Free State, PO Box 339, 9300 Bloemfontein, South Africa
[40] Heisenberg Fellow (DFG), ITA Universität Heidelberg, Germany
[41] GRAPPA, Institute of High-Energy Physics, University of Amsterdam, Science Park 904, 1098 XH Amsterdam, The Netherlands

Appendix A: Additional figures and tables

Additional figures and tables are given here.

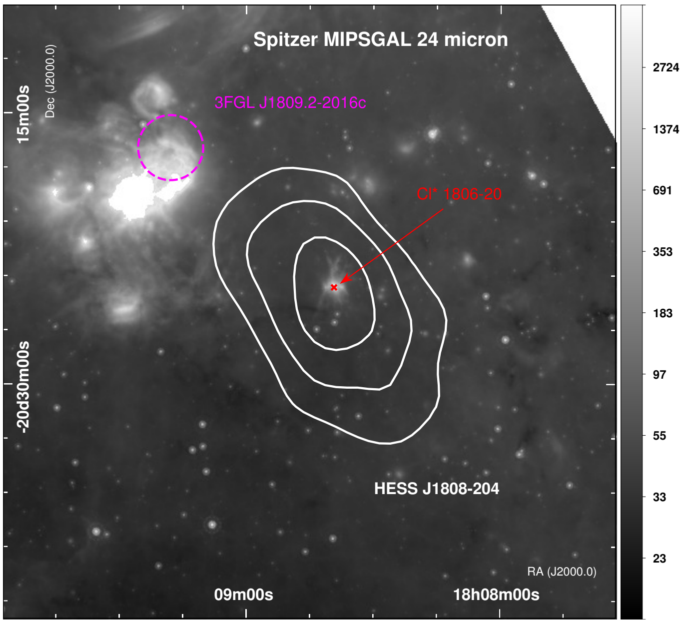

Fig. A.1. *Spitzer* MIPSGAL 24 μm image in MJy/sr units with HESS J1808−204 excess significance contours (6, 5, 4σ as for Fig. 1) overlaid as solid white lines. Locations of the stellar cluster Cl* 1806−20 (containing SGR1806−20 and LBV 1806−20) and the *Fermi*-LAT GeV source 3FGL J1809.2−2016c (68% location error) are indicated. The bright infrared feature to the north-east towards the *Fermi*-LAT source is the W31 giant HII star formation complex.

Table A.1. Event statistics of HESS J1808−204 for events within a radius 0.2° of the fitted position using the reflected background model for both faint and standard cuts analyses.

Events		[1]α	[2]S	Excess events ($N - \alpha N_b$)
– Faint Cuts –				
On (N)	3128			
Off (N_b)	16 758	0.162	7.1σ	412.8
– Standard Cuts –				
On (N)	5147			
Off (N_b)	26 470	0.174	7.4σ	553.4

Notes. 1. Normalisation between on source and background regions. 2. Statistical significance from Eq. (17) of Li & Ma (1983).

Table A.2. VHE spectral fluxes F and 68% statistical error limits of HESS J1808−204 for events within a radius 0.2° of the fitted position using the reflected background model and faint cuts analyses.

E (TeV)	F	F (down) (photons cm^{-2} s^{-1} TeV^{-1})	F (up)
0.34	3.38×10^{-12}	2.39×10^{-12}	4.39×10^{-12}
0.78	5.17×10^{-13}	3.95×10^{-13}	6.42×10^{-13}
2.04	5.10×10^{-14}	3.26×10^{-14}	7.00×10^{-14}
5.35	6.36×10^{-15}	2.80×10^{-15}	1.02×10^{-14}